
Low-Energy (0.1 eV) Electron Attachment S–S Bond Cleavage Assisted by Coulomb Stabilization

AGNIESZKA SAWICKA,^{1,2} JOANNA BERDYS-KOCHAŃSKA,^{1,2}
PIOTR SKURSKI,^{1,2} JACK SIMONS¹

¹ Chemistry Department and Henry Eyring Center for Theoretical Chemistry, University of Utah, Salt Lake City, Utah 84112, USA

² Department of Chemistry, University of Gdansk, Gdansk, Poland

Received 12 September 2004; accepted 13 October 2004

Published online 10 January 2005 in Wiley InterScience (www.interscience.wiley.com).

DOI 10.1002/qua.20449

ABSTRACT: Electron capture by the ion $\text{H}_3\text{C-S-S-CH}_2\text{-CH}_2\text{-NH}_3^+$ at either the $-\text{NH}_3^+$ site (to form the Rydberg radical $\text{H}_3\text{C-S-S-CH}_2\text{-CH}_2\text{-NH}_3$) or into the S–S antibonding σ^* orbital is shown to be able to produce the same S–S bond fragmentation products $\text{H}_3\text{C-S}$ and $\text{HS-CH}_2\text{-CH}_2\text{-NH}_2$, albeit by very different pathways. Capture into the S–S σ^* orbital is, in the absence of the nearby positive site, endothermic by approximately 0.9 eV and leads to an electronically metastable anion that can undergo dissociation or autodetachment. In contrast, in the presence of the stabilizing Coulomb potential provided by the nearby NH_3^+ site, electron attachment into the S–S σ^* orbital is rendered exothermic. As a result, as we have shown in this paper, the effective cross sections for forming the $\text{H}_3\text{C-S}$ and $\text{HS-CH}_2\text{-CH}_2\text{-NH}_2$ products via attachment at the $-\text{NH}_3^+$ and S–S σ^* sites are predicted to be comparable for our model compound. Moreover, we predict that the σ^* site will become more amenable to electron attachment compared with the $-\text{NH}_3^+$ site for compounds in which the distance between the S–S bond and the protonated amine is larger than in our cation. These findings and insights should be of substantial value to workers studying bond cleavage rates and fragmentation patterns in gaseous positively charged samples of peptides and proteins. © 2005 Wiley Periodicals, Inc. *Int J Quantum Chem* 102: 838–846, 2005

Key words: electron attachment; bond cleavage; disulfide bridge

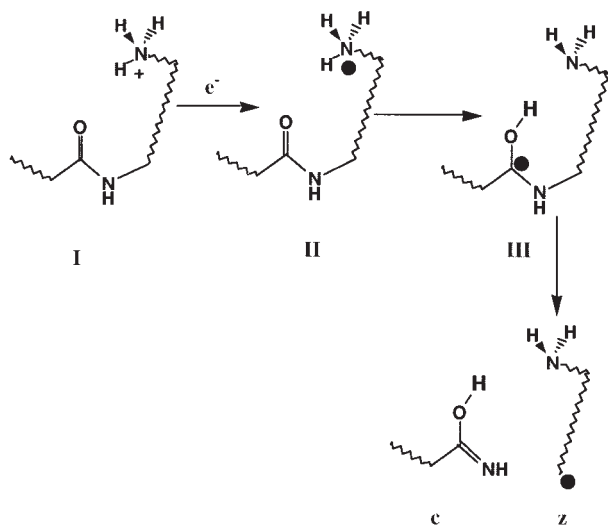
Correspondence to: P. Skurski; e-mail: piotr@hydrogen.hec.utah.edu

Contract grant sponsor: NSF.

Contract grant numbers: 9982420; 0240387.

Contract grant sponsor: Polish State Committee for Scientific Research.

Contract grant number: DS/8371-4-0137-4.



SCHEME 1.

Introduction

The fragmentation patterns produced in mass spectrometric studies of positively charged gas-phase samples of peptides are used to infer the primary structures (i.e., amino acid sequences) of such molecules. Although there exist a variety of methods for effecting fragmentation, a relatively new approach has shown great promise because of its ability to cause very specific (and limited) bond cleavages. Specifically, in electron capture dissociation (ECD) experiments [1], very low-energy electrons are attached to the gaseous sample, after which specific bonds break and thus generate ECD-characteristic fragmentation patterns.

The mechanisms by which electron attachment causes bond cleavage have been the focus of several recent studies [1, 2]. It has been suggested and reasonably well established that the low-energy electrons can be captured at the positive sites (e.g., protonated amines) as a first step in effecting bond cleavages. The hypervalent (sometimes called "Rydberg") $R-NH_3$ radicals thus generated are believed to subsequently release a hydrogen atom that then attacks groups of high H-atom affinity (e.g., carbonyl groups and S-S bonds) to initiate the ECD bond cleavages. An example of such a process is shown in Scheme 1, where the typical fragments are labeled c and z.

Alternative means of dissociating such ions [3] (e.g., collisional activation, electron impact, and infrared multiphoton absorption) tend to fragment

the ions at the C-N bond connecting the carbonyl to its neighboring nitrogen to produce what are termed "b and y fragments."

In an earlier work by this group [4], it was suggested that the ECD electrons may also be captured directly into antibonding σ^* orbitals to cause bond cleavage. Because ECD electron sources contain very low-energy electrons (<1 eV) and because σ^* orbitals usually have high energies, such direct attachments are not to be expected. However, we suggested that those bonds whose σ^* orbital energies are lowered by the Coulomb potentials generated by the positively charged sites can undergo direct dissociative electron attachment. Bonds that have especially low-energy σ^* orbitals are especially susceptible to such attachment processes. In Ref. [4], this suggestion was examined for the situation in which disulfide linkages are broken by direct capture of an electron into an S-S σ^* orbital.

In the current effort, the stabilizing effects of Coulomb potentials due to proximal positive charges are further examined for a small-model molecule that contains a disulfide linkage (whose σ^* orbital is especially low-lying) and a protonated amine site, either of which can serve to capture the ECD electron. The competition for binding an electron to the S-S σ^* orbital or to the $-NH_3^+$ site forms a focus of this study.

OVERVIEW OF OUR PAST WORK

In our first paper on the mechanisms underlying ECD fragmentation, we used our data on a model system to conclude [4] that low-energy electrons (i.e., with kinetic energies near zero) could indeed directly attach to and subsequently fragment S-S σ bonds in disulfide-linked dimers of Ac-Cys-Ala_n-Lys (with n = 10, 15, and 20) that are protonated at their two Lys sites. An example of such a species is shown in Figure 1, where the alanine helices are

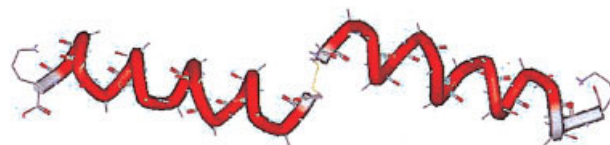


FIGURE 1. Structure of an $(AcCA_{15}K + H)_2^{2+}$ disulfide-linked dimer from (from Ref. [4]). The disulfide linkage is at the center, and the protonated sites are at the left and right termini. [Color figure can be viewed in the online issue, which is available at www.interscience.wiley.com.]

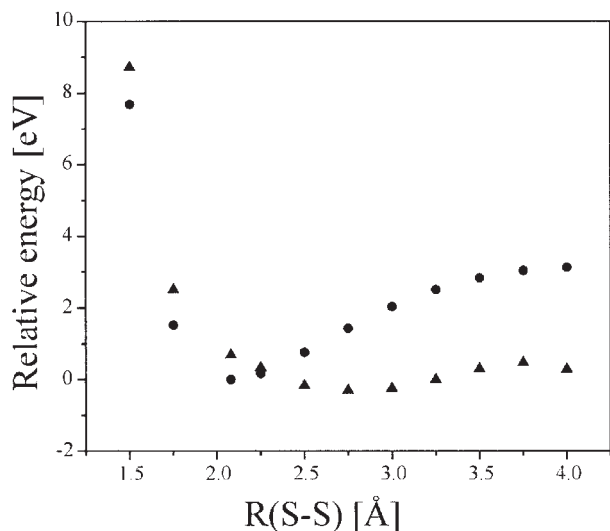


FIGURE 2. Energies of the dimethyl disulfide neutral (circles) and σ^* anion (triangles) as functions of the S-S bond length (\AA) with all other geometrical degrees of freedom relaxed to minimize the energy (taken from Ref. [4]).

shown in red, the cystine linkage containing the S-S bond appears in the center, and the two Lys sites are at the termini.

In the mechanism treated in Ref. [4], an electron enters the S-S antibonding σ^* orbital to form an electronically metastable anion that can either undergo electron autodetachment at a rate of ca. 10^{14} s^{-1} or fragment (promptly, because of the repulsive nature of the σ^* anion's energy surface) to form an $\text{R-S}\cdot$ radical and an $-\text{S-R}$ anion. The yield of bond cleavage is governed by competition between fragmentation on the σ^* surface and autodetachment. The ab initio calculations of Ref. [4] were carried out on a very simple model of the disulfide shown in Figure 1, the $\text{H}_3\text{C-S-S-CH}_3$ molecule. The R-S-S-R' neutral and corresponding anion potential energy curves for dimethyl disulfide as functions of the S-S distance are depicted in Figure 2.

Figure 2 suggests that the near-vertical attachment of an electron into the S-S σ^* orbital of MeS-SMe would require an electron with kinetic energy of ca. 0.9 eV and would generate the σ^* anion on a reasonably repulsive part of its energy surface. This results in the well-known dissociative electron attachment (DEA) process [5] that has been well studied experimentally for MeS-SMe, and the experimental data are in line with our earlier calculations. Figure 2 also suggests that lower-energy electrons (e.g., even zero-energy electrons) can attach to the

σ^* S-S orbital but only if the S-S bond is stretched to near 2.25 \AA , which would require ca. 0.5 eV of vibrational excitation. Of course, except at considerably elevated temperatures, such high vibrational excitation is extremely improbable. So, the most likely means by which electrons can enter the S-S σ^* orbital is to have ca. 0.9 eV of kinetic energy and to do so in a near-vertical manner.

The primary focus in Ref. [4] was to consider the effects that proximal positively charged groups can have on the process in which an electron attaches directly to an S-S σ bond. Specifically, we considered the Coulomb stabilization that one or more nearby positive groups (e.g., the protonated Lys sites in the molecule shown in Fig. 1) can have on the nascent σ^* anion. As an example of the effects of Coulomb interactions, we show in Fig. 3 the MeS-SMe neutral and MeS-SMe $^-$ σ^* anion potentials as in Figure 2 but calculated in the presence of two +1 charges each 30 \AA from the midpoint of the S-S bond (i.e., one +1 charge on one side of the bond, and the other +1 charge in the opposite direction). Clearly, in comparison with Figure 2, the σ^* anion curve in Figure 3 is lowered in energy by a substantial amount relative to the energy of the neutral. This causes the anion curve to intersect the neutral at smaller S-S separations (e.g., at bond lengths that may be accessed in the zero-point vibration of the S-S bond) and at much lower energy.

It turns out that the energy lowering of the σ^* anion curve can be accurately estimated in terms of the Coulomb potential produced by the two +1 charges. For example, when the two charges are 30 \AA distant, the Coulomb energy at the midpoint of the S-S bond is $2 (14.4 \text{ eV } \text{\AA})/30(\text{\AA}) = 0.96 \text{ eV}$; when the two charges are only 10 \AA away, the Coulomb stabilization energy is 2.88 eV. The rigidity of the compounds shown in Figure 1 caused by their helical subunits allowed us to know the distances between the S-S bond and the two +1 sites, so these species provided excellent support for postulate that our model MeS-SMe compounds were designed to probe.

Based upon the results of such studies, we suggested in Ref. [4] that Coulomb potentials produced by nearby positive charges could stabilize the σ^* metastable anion states to an extent that might render them electronically stable. Under such circumstances, the endothermic DEA process illustrated in Figure 2 can be made exothermic or thermoneutral and thus able to effect bond breakage at a much higher yield. The data of Figure 3 suggest that S-S σ bonds, which require electrons of ca. 0.9 eV to

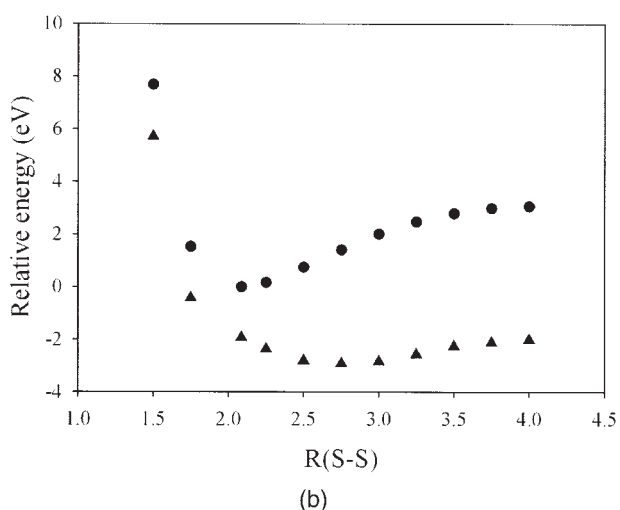
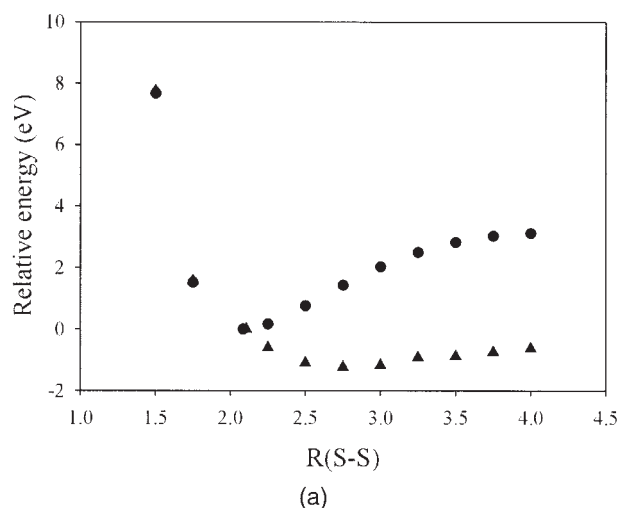


FIGURE 3. Neutral (dots) and σ^* anion (triangles) curves of MeS-SMe in the presence of two +1 charges 30 Å (a) and 10 Å (b) from the midpoint of the S-S bond.

induce DEA in the absence of positive charges, can attach essentially zero-energy electrons if two +1 charges are within 30 Å (or, equivalently, if one +1 charge were within 15 Å) to produce S-S bond cleavage.

THE MODEL COMPOUND STUDIED HERE

In the current work, we extend this earlier effort by considering electron attachment to a model compound shown in Figure 4 that contains both a S-S σ bond and a protonated amine site. We designed this molecule so that the distance from the S-S bond to the positive site was small enough to allow the

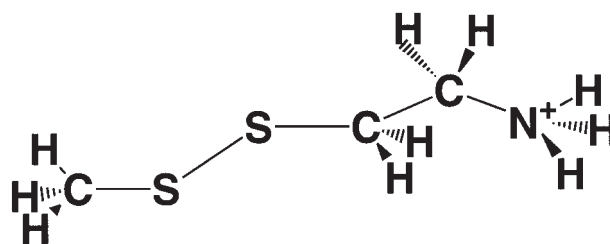
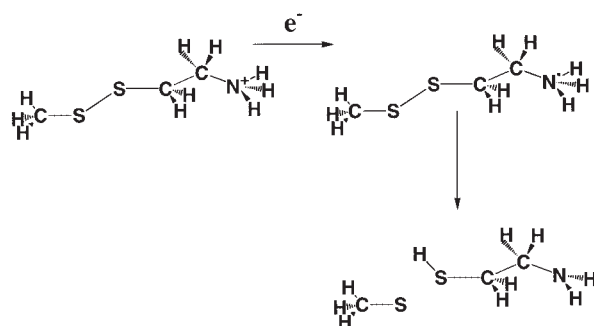


FIGURE 4. Model compound containing S-S σ bond and protonated amine site.

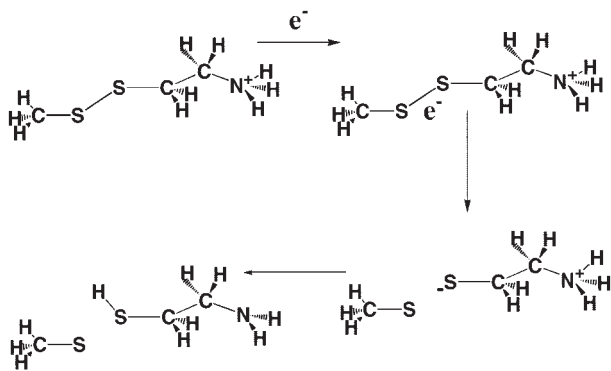
Coulomb potential of the $-\text{NH}_3^+$ site to rendered exothermic direct attachment into the S-S σ^* orbital. For such a molecule, the ECD cleavage of the S-S bond can occur in either of two ways, which form the focus of this work. An electron can be captured at the protonated amine site, followed by H atom attack of the S-S bond (Scheme 2) and SS bond rupture. Alternatively, the electron can be captured at the Coulomb-stabilized S-S bond site, followed by SS bond rupture and intramolecular proton transfer (Scheme 3). In the current work, we examine the energy requirements associated with the electron capture and S-S bond cleavage aspects of these two mechanisms.

Methods

We first optimized the geometry of the cationic species shown in Figure 4 at the second-order Møller-Plesset (MP2) level using aug-cc-pVDZ basis sets [6] with an additional set (5s 5p) of extra diffuse functions [7] centered on the nitrogen atom to properly describe the Rydberg R-NH₃ species. We also calculated all vibrational frequencies to make sure the structure thus found was indeed a



SCHEME 2.



SCHEME 3.

minimum on the energy surface. All of our calculations were carried out using the Gaussian 03 suite [8] of codes. To generate the cation and neutral-molecule energies as functions of the S–S bond length (R), we performed unrestricted MP2 (UMP2) calculations at a range of R -values with all other geometrical degrees of freedom relaxed to minimize the electronic energy. Because the methods we used are based on an unrestricted Hartree–Fock starting point, it is important to make sure that little if any artificial spin contamination enters into the final wavefunctions. We computed the expectation value $\langle S^2 \rangle$ for species studied in this work and found values not exceeding 0.830 (after annihilation) in all open-shell doublet neutral cases. It should be noted that the spin contamination is substantially smaller (ca. 0.77) when the electron is occupying the S–S σ^* orbital (compared with the species with an electron attached to the $-\text{NH}_3^+$ site), and it increases along the dissociation potential energy curve (although it does not exceed the reported values). The unrestricted calculations were necessary to achieve a qualitatively correct description of the hemolytic cleavage of the S–S bond and because some of the molecules we studied are open-shell species. For the neutral molecule, we computed the energies of two different electronic states: one with an electron attached to the $-\text{NH}_3^+$ site to generate a hypervalent radical and another with an electron occupying the S–S σ^* orbital.

Results and Discussion

RELEVANT POTENTIAL ENERGY CURVES

As a result of such a treatment, we were able to compute the electronic energies of the cation and of

the neutral molecule as functions of the S–S bond length. In particular, we were able to evaluate the σ^* neutral's energy and the energy of the neutral species in which a hypervalent $-\text{NH}_3$ site holds an excess electron at all R -values. In Figure 5 we show the potential energy curves for these three species, and we label four species 1–4 whose role in the bond cleavage process we discuss below.

The following observations can be made about the data in Figure 5:

1. The cation and hypervalent neutral have very similar equilibrium geometries. This, of course, is expected based on our experience with such species [9] in which the attached electron occupies a nonbonding Rydberg-like orbital;
2. The hypervalent neutral lies ca. 4 eV below the cation at the latter's equilibrium geometry for all R -values out to the large- R asymptote. This also is not surprising, because the energy associated with adding an electron to the $-\text{NH}_3^+$ site is affected little by the presence or absence of the rather distant S–S bond;
3. The σ^* neutral lies ca. 2 eV below the cation at

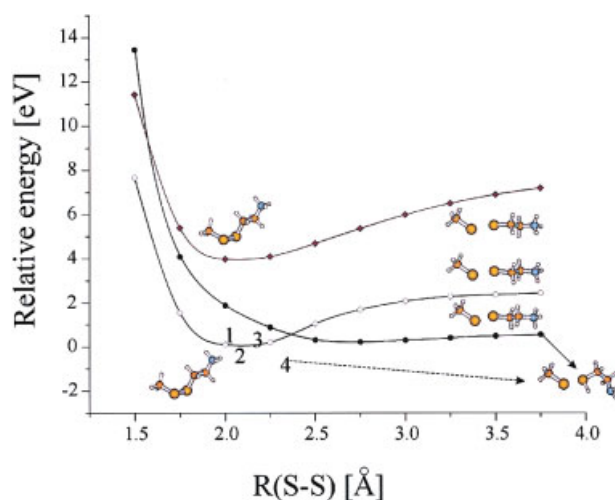
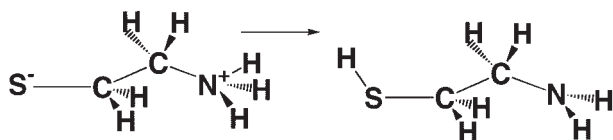


FIGURE 5. Cation (triangles), hypervalent amine neutral (open circles), and σ^* S–S neutral (filled circles) energies as functions of the S–S bond length. Also shown are the structures of the various species at the minima and asymptotes. The numbers 1–4 represent species on the pathway connecting the hypervalent $\text{H}_3\text{C}-\text{S}-\text{S}-\text{CH}_2-\text{CH}_2-\text{NH}_3$ with the $\text{H}_3\text{C}-\text{S}$ and $\text{HS}-\text{CH}_2-\text{CH}_2-\text{NH}_2$ products (see text). [Color figure can be viewed in the online issue, which is available at www.interscience.wiley.com.]



SCHEME 4.

the cation's equilibrium S-S bond length. We know from our past work [4] on MeS-SMe that such S-S σ^* states lie ca. 1 eV above the corresponding neutral in the absence of any Coulomb stabilization. So, the fact that the σ^* state lies 2 eV below the cation in the current case means that the energy of the S-S σ^* state has been lowered by the Coulomb potential produced by the protonated amine site;

- The hypervalent neutral is energetically more stable than the σ^* neutral at the cation's equilibrium geometry, but the latter is more stable at large R (i.e., once the S-S bond is ruptured);
- Once the S-S bond has fully broken on the σ^* neutral potential surface, the $^-S-CH_2-CH_2-NH_3^+$ species spontaneously undergoes a 2.0-eV exothermic intramolecular proton transfer, as shown in Scheme 4, to form the neutral HS-CH₂-CH₂-NH₂, shown at the lower right of Figure 5;
- It is known [10] that the Rydberg neutral CH₃-S-S-CH₂-CH₂-NH₃ can eject an H atom by overcoming a very small (ca. 0.1 eV) barrier (shown by the number 1 in Fig. 5) to form CH₃-S-S-CH₂-CH₂-NH₂ + H (number 2 in Fig. 5), which lies ca. 0.1 eV below the Rydberg neutral;
- If the ejected H atom traverses in a direction that causes it to strike the S-S bond, it can attach to one of the S atoms by overcoming a small (ca. 0.1 eV [11]) barrier (number 3 in Fig. 5) to form CH₃-S-SH-CH₂-CH₂-NH₂. The latter species (number 4 in Fig. 5) lies ca. 1 eV below CH₃-S-S-CH₂-CH₂-NH₂ + H [12] and thus has enough internal energy to promptly cleave its S-S bond [13] and decay to HS-CH₂-CH₂-NH₂ + CH₃-S, which is shown at the lower right of Figure 5.

The final products generated by electron attachment to either the $-NH_3^+$ site or the S-S σ^* orbital are therefore identical; cleavage of the S-S bond produces HS-CH₂-CH₂-NH₂ + CH₃-S. However, it is important to address the issue of what fraction

of the reactions proceed through attachment at the $-NH_3^+$ site and what fraction involve formation of the σ^* neutral.

BRANCHING RATIOS IN THE ELECTRON ATTACHMENT PROCESSES

We now consider what happens when low-energy electrons strike a cation such as that shown in Figure 4. A full theoretical simulation of the electron capture process would involve solving quantum scattering equations for the electron moving in the potential presented by this cation. The potential is attractive in regions of space near the $-NH_3^+$ site and near the S-S σ^* orbital [14], and the relative abilities of these two regions to bind the incident electron are critical to understanding the branching ratios for $-NH_3^+$ and σ^* attachment. A rigorous quantum electron scattering approach is beyond our capabilities at present. However, we believe that much can be said about how the capture and subsequent S-S bond fragmentation likely occur by combining information shown in Figure 5 with independent experimental and theoretical data.

Attachment to the $-NH_3^+$ Site

Let us first consider electron attachment to the $-NH_3^+$ site. Unfortunately, very few absolute cross sections have been determined for electron attachment to cations, and, to the best of our knowledge, this cross section is not known for our model compound. It is known [15] that the cross section for attachment of 0.1 eV electrons [16] to a cation site such as $OH_3^+ + e^- \rightarrow OH_3$ is of the order of 10^{-14} cm². It is believed that the process occurs by initial capture into a high Rydberg state of the OH₃ radical followed by radiationless relaxation to lower electronic states. Moreover, the cross section for $SH_3^+ + e^- \rightarrow SH_3$ is also ca. 10^{-14} cm², so it seems reasonable to assume that the $-NH_3^+ + e^- \rightarrow -NH_3$ cross section is in this same range.

After the $-NH_3$ radical is formed, it can undergo loss of an H atom (species 3 in Fig. 5) in a few microseconds with the ejected H atom having a kinetic energy of ca. 0.1 eV. Assuming that the H atoms are ejected isotropically [17] relative to the S-S bond, only a fraction of these H atoms will be directed toward the S-S bond. The fraction of H atoms that strike the S-S bond can be estimated knowing the distance R from the S-S bond midpoint to the ejected H atom and the length R_{SS} of the S-S bond. A sphere of radius R has area πR^2 and the

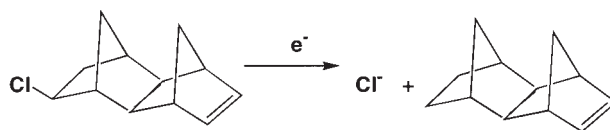
S-S bond region covers an area of approximately $\pi(R_{SS}/2)^2$, so the fraction of ejected H atoms likely to strike the S-S bond is $(R_{SS}/2R)^2$. Using $R_{SS} = 2 \text{ \AA}$ and $R = 5 \text{ \AA}$ (the distance from the midpoint of the S-S bond and the nitrogen atom in the equilibrium geometry of $\text{H}_3\text{C-S-S-CH}_2\text{-CH}_2\text{-NH}_3^+$), we estimate that 4% of the ejected H atoms will strike the S-S bond for our model compound [18].

Of the ca. 4% of H atoms that strike the S-S bond, only a fraction will react to produce the S-H bond adduct $\text{H}_3\text{C-S-SH-CH}_2\text{-CH}_2\text{-NH}_2$. It was shown in Ref. [11] that addition of an H atom to the -S-S-bond requires surmounting a 0.1 to 0.4 eV barrier, depending on the orientation at which the H atom strikes the S-S bond. Knowing that the H atoms possess ca. 0.1 eV of kinetic energy, we could thus estimate the fraction of collisions with the S-S bonds that produce $\text{H}_3\text{C-S-SH-CH}_2\text{-CH}_2\text{-NH}_2$ if we know how much of the angular space surrounding each S-S bond has the minimum barrier of 0.1 eV. Unfortunately, this issue was not addressed in Ref. [11], but based on an examination of the 0.1 eV transition state structure shown in Figure 1 of ref. 11, it seems clear that the H atom must interact with one of the sulfur lone pair orbitals. It seems reasonable to estimate the fraction of angular space occupied by these orbitals to be in the 10–50% range.

The 4% of H atoms that can strike the S-S bond combined with the 10–50% of these that strike the S-S bond at angles that can successfully lead to an S-H bond and the 10^{-14} cm^2 electron attachment cross section suggest that the effective cross section for forming $\text{H}_3\text{C-S-SH-CH}_2\text{-CH}_2\text{-NH}_2$ by electron attachment to the $-\text{NH}_3^+$ site should be in the $4 \times 10^{-17} \text{ cm}^2$ to $2 \times 10^{-16} \text{ cm}^2$ range. If we then assume that $\text{H}_3\text{C-S-SH-CH}_2\text{-CH}_2\text{-NH}_2$ can spontaneously decompose to $\text{H}_3\text{C-S} + \text{SH-CH}_2\text{-CH}_2\text{-NH}_2$, this range of cross sections should also relate to the formation of the final fragmentation products via the $-\text{NH}_3^+$ attachment route.

Attachment to the S-S σ^* Site

We now consider the alternative route for forming $\text{H}_3\text{C-S} + \text{SH-CH}_2\text{-CH}_2\text{-NH}_2$, by the electron attaching directly to form the σ^* state of the neutral. Again we face a situation in which the absolute cross section for attaching an electron to the σ^* orbital and realizing cleavage of the S-S bond for our compound is not known. We therefore must make a reasonable estimate of this cross section, as well. The cross section for $\text{CHF}_2\text{Cl} + e^- \rightarrow \text{Cl}^- + \text{CHF}_2$ has been determined to be $2 \times 10^{-19} \text{ cm}^2$ [19],



SCHEME 5.

which reflects the cross section for electron capture multiplied by the fraction F of nascent $(\text{CHF}_2\text{Cl})^- \sigma^*$ anions that survive long enough for their C-Cl bond to rupture. This fraction is governed by the rate k_{diss} at which the C-Cl bond breaks (in ca. $1/2$ a vibrational period or at 10^{14} s^{-1}) and the rate k_{detach} at which the σ^* anion undergoes electron autodetachment (ca. 10^{15} s^{-1}): $F = k_{\text{diss}}/(k_{\text{diss}} + k_{\text{detach}}) \approx 10^{-1}$ in the C-Cl bond rupture case. This means that the cross section for electron capture is in the $2 \times 10^{-18}\text{-cm}^2$ range for CHF_2Cl . It is the latter type of cross section (i.e., with the fraction F removed) that is pertinent to our case because electron capture into the S-S σ^* orbital of the cation shown in Figure 4 does not lead to an electronically metastable state that can undergo autodetachment because the Coulomb potential of the nearby $-\text{NH}_3^+$ group renders this σ^* state electronically bound.

Another example of a known cross section for dissociative electron attachment is that for the process shown in Scheme 5, which is [20] $7 \times 10^{-18} \text{ cm}^2$. Again, this cross section relates to the attachment (to the olefin π^* orbital) followed by the cleavage of the C-Cl σ bond, so it must be corrected for the fraction F of nascent π^* anions that survive long enough to break the C-Cl bond. This fraction is also in the 10^{-1} range; so for Scheme 5 the cross section for attachment alone is approximately $7 \times 10^{-17} \text{ cm}^2$.

Competition among Attachment Processes

Based on our analysis thus far, we expect that:

- Attachment of a 0.1 eV electron to the $-\text{NH}_3^+$ site, followed by H-atom ejection and attack of an H atom on a -S-S-bond to form -S-SH- and bond cleavage to generate -S + HS- should occur with an effective cross section in the 4×10^{-17} - to $2 \times 10^{-16}\text{-cm}^2$ range.
- Attachment of a low-energy electron to the S-S σ^* orbital followed by bond cleavage and eventual intramolecular proton transfer to form the same -S + HS-species should

have an effective cross section in the 2×10^{-18} - to 7×10^{-17} -cm² range.

These conclusions suggest that bond cleavage effected via attachment to the $-\text{NH}_3^+$ site should be more prevalent than cleavage initiated by σ^* electron capture. However, there are two aspects of the processes discussed above that we still need to address:

- (a) The fraction of H atoms that are directed toward the SS bond decays as R^{-2} , where R is the distance from the middle of the SS bond and the $-\text{NH}_3^+$ site. For our model compound, $R = 5 \text{ \AA}$. However, for compounds with more distant positive sites (e.g., for $R = 10$ or 15 \AA), the fractions and thus the effective cross sections are reduced by factors of 4 and 9, respectively. This means that for compounds with the positively charged sites further from the SS bond [18], the branching ratio for bond cleavage initiated by electron attachment to the $-\text{NH}_3^+$ site should be substantially less than for our model compound.
- (b) The cross sections that we quoted above for attachment to σ^* orbitals, even after being corrected for the fraction that dissociate versus those that undergo autodetachment, are probably lower limits. This is true because the data we quoted relate to attaching electrons to neutral molecules (i.e., to CHF_2Cl or to the compound shown in Scheme 5) to form electronically metastable anions; such processes require the electron to have significantly larger (e.g., 1 eV) kinetic energies than are common in ECD experiments. Our compound's σ^* orbital is electronically stable and thus can attach much lower-energy electrons. We know [19, 21] that electron attachment cross sections to neutral molecules vary with electron energy as $E^{-1/2}$, whereas cross sections for attaching to cations vary [21] as E^{-1} . So, for the 0.1 eV electrons we have been considering here, the σ^* attachment cross sections are probably three to 10 times larger than what we inferred from the 1 eV data.
- (c) Moreover, although the effective cross sections for proceeding via the $-\text{NH}_3^+$ route fall off as R^{-2} , the Coulomb stabilization of the σ^* state decays as R^{-1} . Therefore, even when $R = 10 \text{ \AA}$ or 15 \AA , the σ^* state remains elec-

tronically stable, which means the effective cross section for σ^* attachment should remain nearly constant over this range of R values, whereas that for $-\text{NH}_3^+$ attachment should decay.

Summary

We have used ab initio electronic structure calculations on a model cation and two of its daughter neutral-molecule states accessed by attaching an electron to the cation to address the relative rates of attachment to two sites in the cation. The importance of this work lies primarily in its ability to provide insight into two competing pathways by which low-energy electrons attach to and subsequently fragment gas-phase positively charged samples of peptides and proteins.

Our calculations pertaining to low-energy (i.e., 0.1 eV) electron attachment to the model compound $\text{H}_3\text{C-S-S-CH}_2\text{-CH}_2\text{-NH}_3^+$ to produce S-S bond cleavage and generate $\text{H}_3\text{C-S}$ and $\text{HS-S-CH}_2\text{-CH}_2\text{-NH}_2$ suggest that:

- (1) Capture at the $-\text{NH}_3^+$ and S-S σ^* orbital sites have cross sections in the ranges of 4×10^{-17} cm² to 2×10^{-16} cm² and three to 10 times (2×10^{-18} to 7×10^{-17} cm²), respectively, for our model compound, in which the SS and $-\text{NH}_3^+$ sites are separated by ca. 5 \AA . We therefore expect the branching ratio for attaching to these two sites to be similar in magnitude for this particular ion.
- (2) For species in which the SS and $-\text{NH}_3^+$ sites are separated by larger distances R, the cross section for proceeding through the $-\text{NH}_3^+$ site should fall off as R^{-2} . That for the SS σ^* site should be much less R-dependent as long as the Coulomb stabilization [14.4 eV $\text{\AA}/R$ (\AA)] renders the SS σ^* orbital electronically stable. Because the SS σ^* state is ca. 0.9 eV unstable in the absence of any Coulomb potential, this means that R must remain below ca. 15 \AA for the SS site to be able to exothermically attach electrons. For this reason, we expect attachment to the SS σ^* site to be more likely in compounds where the positive sites are 5–15 \AA apart.

The results presented here should be tested in the laboratory by carrying out electron-capture dis-

sociation experiments on compounds that contain SS bonds and protonated amine sites separated by rigid spacer groups that keep the distance between these two groups fixed. The data from such experiments would allow for evaluation of our predictions about the distance dependence of the relative rates.

ACKNOWLEDGMENTS

This work was supported by NSF, grant numbers 9982420 and 0240387 (to J.S.) and by the Polish State Committee for Scientific Research (K.B.N.), grant number DS/8371-4-0137-4 (to P.S.). Significant computer time provided by the Center for High Performance Computing at the University of Utah and by the Academic Computer Center in Gdansk (TASK) is also gratefully acknowledged.

References

- Zubarev, R.; Kruger, N.; Fridriksson, E. K.; Lewis, M. A.; Horn, D. M.; Carpenter, B. K.; McLafferty, F. W. *J Am Chem Soc* 1999, 121, 2857–2862; Zubarev, R. A.; Horn, D. M.; Fridriksson, E. K.; Kelleher, N. L.; Kruger, N. A.; Lewis, M. A.; Carpenter, B. K.; McLafferty, F. W. *Anal Chem* 2000, 72, 563–573.
- Syrstad, E. A.; Turecek, F. *J Phys Chem A* 105, 2001, 11144–1115; Turecek, F.; Syrstad, E. A. *J Am Chem Soc* 2003, 125, 3353–3369; Turecek, F.; Polasek, M.; Frank, A.; Sadilek, M. *J Am Chem Soc* 2000, 122, 2361–2370; Hudgins, R. R.; Håkansson, K.; Quinn, J. P.; Hendrickson, C. L.; Marshall, A. G. Proceedings of the 50th ASMS Conference on Mass Spectrometry and Allied Topics, Orlando, Florida, June 2–6, 2002.
- Kruger, N. A.; Zubarev, R. A.; Carpenter, B. K.; Kelleher, N. L.; Horn, D. M.; McLafferty, F. W. *Inter J Mass Spectrosc* 1999, 182/183, 1–5.
- Sawicka, A.; Skurski, P.; Hudgins, R. R.; Simons, J. *J Phys Chem B* 107, 2003, 13505–13511.
- Dezarnaud-Dandine, C.; Bournel, F.; Tronc, M.; Jones, D.; Modelli, A. *J Phys B At Mol Opt Phys* 1998, 31, L497–L501; Modelli, A.; Jones, D.; Distefano, G.; Tronc, M. *Chem Phys Lett* 1991, 181, 361–366.
- Kendall, R. A.; Dunning, T. H., Jr.; Harrison, R. J. *J Chem Phys* 1992, 96, 6796.
- Gutowski, M.; Simons, J. *J Chem Phys* 1990, 93, 3874; Skurski, P.; Gutowski, M.; Simons, J. *Int J Quantum Chem* 2000, 80, 1024–1038.
- Frisch, M. J.; Trucks, G. W.; Schlegel, H. B.; Scuseria, G. E.; Robb, M. A.; Cheeseman, J. R.; Montgomery, J. A. Jr.; Vreven, T.; Kudin, K. N.; Burant, J. C.; Millam, J. M.; Iyengar, S. S.; Tomasi, J.; Barone, V.; Mennucci, B.; Cossi, M.; Scalmani, G.; Rega, N.; Petersson, G. A.; Nakatsuji, H.; Hada, M.; Ehara, M.; Toyota, K.; Fukuda, R.; Hasegawa, J.; Ishida, M.; Nakajima, T.; Honda, Y.; Kitao, O.; Nakai, H.; Klene, M.; Li, X.; Knox, J. E.; Hratchian, H. P.; Cross, J. B.; Adamo, C.; Jaramillo, J.; Gomperts, R.; Stratmann, R. E.; Yazyev, O.; Austin, A. J.; Cammi, R.; Pomelli, C.; Ochterski, J. W.; Ayala, P. Y.; Morokuma, K.; Voth, G. A.; Salvador, P.; Dannenberg, J. J.; Zakrzewski, V. G.; Dapprich, S.; Daniels, A. D.; Strain, M. C.; Farkas, O.; Malick, D. K.; Rabuck, A. D.; Raghavachari, K.; Foresman, J. B.; Ortiz, J. V.; Cui, Q.; Baboul, A. G.; Clifford, S.; Cioslowski, J.; Stefanov, B. B.; Liu, G.; Liashenko, A.; Piskorz, P.; Komaromi, I.; Martin, R. L.; Fox, D. J.; Keith, T.; Al-Laham, M. A.; Peng, C. Y.; Nanayakkara, A.; Challacombe, M.; Gill, P. M. W.; Johnson, B.; Chen, W.; Wong, M. W.; Gonzalez, C.; Pople, J. A. *Gaussian 03, Revision A.1*; Gaussian: Pittsburgh, 2003.
- Gutowski, M.; Taylor, H.; Hernandez, R.; Simons, J. *J Phys Chem* 1988, 92, 6179–6182; Gutowski, M.; Simons, J. *J Chem Phys* 1990, 93, 3874–3880; Simons, J.; Gutowski, M. *Chem Rev* 1991, 91, 669–677; Boldyrev, A. I.; Simons, J. *J Chem Phys* 1992, 97, 6621–6627; Boldyrev, A. I.; Simons, J. *J Phys Chem* 1992, 96, 8840–8843; Boldyrev, A. I.; Simons, J. *J Phys Chem A* 1999, 103, 3575–3580; Ketvirtis, A.; Simons, J. *J Phys Chem* 1999, 103, 6552–6563.
- Raynor, S.; Herschbach, D. R. *J Phys Chem* 1982, 86, 3592; Gelene, G. I.; Cleary, D. A.; Porter, R. *J Chem Phys* 1982, 11, 3311.
- Turecek, F.; Polasek, M.; Frank, A. J.; Sadilek, M. *J Am Chem Soc* 2000.
- It has been shown (Ref. [11]) that $\text{CH}_3\text{-SS-CH}_3 + \text{H} \rightarrow \text{CH}_3\text{SSH-CH}_3$ is exothermic by 96 kJ mol^{-1} , so we assume approximately this energy balance for $\text{CH}_3\text{-S-S-CH}_2\text{-CH}_2\text{-NH}_2 + \text{H} \rightarrow \text{CH}_3\text{-S-SH-CH}_2\text{-CH}_2\text{-NH}_2$.
- In Ref. [11] it was shown that $\text{CH}_3\text{SSH-CH}_3 \rightarrow \text{CH}_3\text{S} + \text{SH-CH}_3$ was endothermic by 8 kJ mol^{-1} .
- It is obvious that the potential is attractive near the positive site of the cation. That it is also attractive near the S–S antibonding orbital can be inferred from the fact that the σ^* electronic state of the neutral as shown in Figure 5 lies below the energy of the cation in regions of S–S bond lengths near the cation's equilibrium geometry.
- Vejby-Christensen, L.; Andersen, L. H.; Heber, O.; Kella, D.; Pedersen, H. B.; Schmidt, H. T.; Zajfman, D. *Astrophys J* 1997, 483, 531–540.
- We choose this electron energy because it is characteristic of the low-energy electron capture dissociation experiments to which we are trying to relate.
- Certainly the N–H bonds are directed, but the distribution of orientations of the ruptured N–H bond relative to the S–S bond whose eventual cleavage we consider here is likely isotropic because of the flexibility of the $-\text{CH}_2\text{-CH}_2\text{-NH}_3$ chain.
- Of course, this fraction fluctuates as the $-\text{CH}_2\text{-CH}_2\text{-NH}_3^+$ chain moves and can be larger if the chain is folded toward the SS group and can be smaller for longer chain lengths.
- Cicman, P.; Pelc, A.; Sailer, W.; Matejcek, S.; Scheier, P.; Mark, T. *Chem Phys Lett* 2003, 371, 231–237. This cross section was determined for 1.1-eV electrons; it is known (see D. Klar, M.-W. Ruf, I. I. Fabrikant, and H. Hotop, *J Phys B* 2001, 34, 3855–3878) that the cross section varies with electron energy E approximately as $E^{-1/2}$. So, for electrons having kinetic energy in the 0.1-eV range, as we are considering here, the cross section is expected to be somewhat larger than that stated here.
- Pearl, D. M.; Burrow, P. D.; Nash, J. J.; Morrison, H.; Nachtigalova, D.; Jordan, K. D. *J Phys Chem* 1999, 99, 12379–12381.
- Wigner, E. P. *Phys Rev* 1948, 73, 1002.